



Published in final edited form as:

*Circ Cardiovasc Interv.* 2016 October ; 9(10): . doi:10.1161/CIRCINTERVENTIONS.116.004058.

## Injectable Shear-Thinning Hydrogels for Minimally Invasive Delivery to Infarcted Myocardium to Limit Left-Ventricular Remodeling

Christopher B. Rodell, PhD<sup>1</sup>, Madonna E. Lee, MD<sup>2</sup>, Hua Wang, BS<sup>3</sup>, Satoshi Takebayashi, MD<sup>2</sup>, Tetsushi Takayama, MD<sup>2</sup>, Tomonori Kawamura, MD<sup>2</sup>, Jeffrey S. Arkles, MD<sup>2</sup>, Neville N. Dusaj, MS<sup>1</sup>, Shauna M. Dorsey, PhD<sup>1</sup>, Walter R.T. Witschey, PhD<sup>4</sup>, James J. Pilla, PhD<sup>4</sup>, Joseph H. Gorman III, MD<sup>2</sup>, Jonathan F. Wenk, PhD<sup>3,5</sup>, Jason A. Burdick, PhD<sup>1,\*</sup>, and Robert C. Gorman, MD<sup>2,\*</sup>

<sup>1</sup>Department of Bioengineering, University of Pennsylvania, Philadelphia, Pennsylvania

<sup>2</sup>Gorman Cardiovascular Research Group, Department of Surgery, University of Pennsylvania, Philadelphia, Pennsylvania

<sup>3</sup>Department of Mechanical Engineering, University of Kentucky, Lexington, Kentucky

<sup>4</sup>Department of Radiology, University of Pennsylvania, Philadelphia, Pennsylvania

<sup>5</sup>Department of Surgery, University of Kentucky, Lexington, Kentucky

### Abstract

**Background**—Injectable, acellular biomaterials hold promise to limit left ventricular (LV) remodeling and heart failure precipitated by infarction through bulking and/or stiffening the infarct region. A material with tunable properties (e.g., mechanics, degradation) that can be delivered percutaneously has not yet been demonstrated. Catheter deliverable soft hydrogels with *in vivo* stiffening to enhance therapeutic efficacy achieve these requirements.

**Methods and Results**—We developed a hyaluronic acid hydrogel that utilizes a tandem crosslinking approach, where the first crosslinking (guest-host, GH) enabled injection and localized retention of a soft (<1kPa) hydrogel. A second crosslinking reaction (dual-crosslinking, DC) stiffened the hydrogel (41.4±4.3kPa) after injection. Posterolateral infarcts were investigated in an ovine model (n = 6 per group), with injection of saline (MI control), GH, or DC.

Computational (day 1), histological (1 day, 8 wk), morphological and functional (0, 2, 8 wk) outcomes were evaluated. Finite element modeling projected myofiber stress reduction (>50%, P<0.001) with DC but not GH injection. Remodeling, assessed by infarct thickness and LV volume, was mitigated by hydrogel treatment. Ejection fraction was improved, relative to MI at 8 weeks, with DC (37% improvement, P=0.014) and GH (15% improvement, P=0.058) treatments.

\*Corresponding Authors: Jason A. Burdick, Ph.D., University of Pennsylvania, Suite 240, Skirkanich Hall, 210 S. 33<sup>rd</sup> Street, Philadelphia, PA 19104, burdick2@seas.upenn.edu, Phone: 215-898-8537; Fax: 215-573-2071, or Robert C. Gorman, MD, Gorman Cardiovascular Research Group, Smilow Center for Translational Research, 3400 Civic Center Blvd – Building 421, 11th Floor, Room 112, Philadelphia, PA 19104, Robert.Gorman@uphs.upenn.edu, Phone: 215-746-5156; Fax: 215-746-7415.

**Disclosures**  
None.

Percutaneous delivery via endocardial injection was investigated with fluoroscopic and echocardiographic guidance, with delivery visualized by MRI.

**Conclusions**—A percutaneous delivered hydrogel system was developed, and hydrogels with increased stiffness were most effective in ameliorating LV remodeling and preserving function. Ultimately, engineered systems such as these have the potential to provide effective clinical options to limit remodeling in patients after infarction.

### Keywords

heart failure; myocardial infarction; remodeling; percutaneous treatment; hydrogel

---

In the United States, an estimated 785,000 acute myocardial infarctions (MIs) occur annually, and the speed of treatment and use of percutaneous coronary interventions have improved the in hospital survival rate by nearly 40% in recent decades.<sup>1,2</sup> However, there remain downstream consequences for these patients, as MI is known to be a major contributor to the development of chronic heart failure (HF), which affects an estimated 5.7 million Americans.<sup>1</sup> Transplantation remains the only definitive treatment for HF, motivating the development of preventative therapies.

In the case of ischemic HF, loss of LV function is the result of LV remodeling through a deleterious cascade of biological and mechanical events, which ultimately result in geometric reshaping of the LV and loss of contractile function.<sup>3–5</sup> It has been recognized that infarct compliance plays a major role in this process, as loss of infarct contractility results in increased systolic compliance, creating an energy sink which increases workload on the remaining healthy tissue.<sup>4</sup> Moreover, passive mechanical properties of the infarct are reduced for as long as 6 weeks,<sup>6</sup> largely as a result of a spatiotemporal imbalance of matrix metalloproteinase activity favoring proteolysis.<sup>7</sup> Due to these changes, the infarct is susceptible to energetic losses, thinning, and planar expansion in early stages post-MI, contributing to abnormal stress distributions and continued detriment to the borderzone contractility,<sup>8,9</sup> which perpetuate ventricular dilation.

To counter the effects of infarct expansion, mechanical interventions early post-MI are of great utility, including affixed patches or wraps that act as restraints and biomaterial injection to stabilize the infarct.<sup>10</sup> While effective in preclinical studies, therapeutic approaches that require thoracotomy for the application of restraints will likely not achieve widespread application due to risks associated with thoracic surgery early after MI. Thus, the use of biomaterials to mechanically stabilize the infarct is attractive, in part, because of the potential for minimally invasive percutaneous delivery. Numerous injectable hydrogels have been investigated, spanning a wide range of material properties and methods of delivery<sup>11</sup> and prior studies have demonstrated the importance of the material mechanical properties<sup>12</sup> and prolonged degradation<sup>13</sup> on remodeling outcomes.

Despite the need for minimally invasive techniques for hydrogel delivery, only a few currently available hydrogels (e.g., decellularized ECM, alginate) have been delivered via intracoronary or intramyocardial injection.<sup>14–16</sup> While they have proceeded to clinical trials, the modest stiffness of these materials (10 Pa for decellularized ECM)<sup>17</sup> make them

unsuitable for mechanical stabilization of the infarct. It has been demonstrated that supraphysiological hydrogel moduli of approximately 40 kPa effectively attenuate LV remodeling.<sup>12</sup> To address this need, we have developed an injectable hydrogel system based on guest-host (GH) interactions that is shear-thinning (i.e., flows easily through a syringe or catheter) and self-healing (i.e., localizes at the injection site). The hydrogel includes an optional secondary crosslinking (DC) that occurs *in situ* to enhance mechanical properties (approximately 40kPa moduli, motivated by prior results) and prolong degradation. Herein, we demonstrate the utility of these material systems toward attenuating the LV remodeling response post-MI and demonstrate the feasibility of percutaneous hydrogel delivery in an ovine model.

## METHODS

### Hydrogel synthesis and preparation

Modified hyaluronic acid (HA) polymers were prepared by methods previously described, as detailed in supplementary methods.<sup>18, 19</sup> These included HA modified with adamantane (Ad-HA) or  $\beta$ -cyclodextrin (CD-HA) to form guest-host (GH) hydrogels, as well as HA modified with both adamantane and thiols (Ad-HA-SH) or both  $\beta$ -cyclodextrin and methacrylates (CD-MeHA) to form dual-crosslinking (DC) hydrogels. GH hydrogels were formed under sterile conditions by dissolution of the two polymers in PBS at (4.5wt%), mixing of the two solutions, and loading into syringes for injection. Adamantane (guest, Ad) and  $\beta$ -cyclodextrin (host, CD) were present in equimolar ratios, and the concentration denotes the combined weight percent of both polymers in solution. DC hydrogels were similarly prepared, with the pH of buffers adjusted to obtain a pH=5.

### *In vitro* hydrogel evaluation

To assess hydrogel mechanical properties, oscillatory rheology was performed (AR2000, TA Instruments; 20 mm diameter cone-plate, 59 min 42 s angle, 27  $\mu$ m gap, 37°C). GH hydrogel mechanics were determined by frequency (0.01–100 Hz; 1.0% strain) and strain sweeps (1.0 Hz; 0.1–500% strain). Compressive mechanical analysis (Q800, TA Instruments) of DC hydrogels was performed serially on samples (n = 6) following overnight crosslinking at 37°C with a rate of 10% strain/min (moduli were calculated from 10–20% strain).

To examine hydrogel degradation, 30  $\mu$ L hydrogels (n = 5) were contained within a 5 mm diameter depression in acrylamide molds. Hydrogels were submerged in 1 mL PBS and stored at 37°C. At set time points, the buffer was collected and replaced. At study completion, hydrogels were degraded in hyaluronidase (1.0 mg/mL) to determine remaining hydrogel content. Degradation was quantified via a uronic acid assay with normalization to cumulative release.

### Finite-Element (FE) modeling

FE modeling of end-diastolic myocardial thickness and corresponding myofiber stress distributions was conducted by adaptation of a method similar to those previously described, as detailed in the supplementary methods.<sup>20</sup> Briefly, the LV geometry was approximated by an ellipsoidal model and hydrogel inclusions introduced to displace the myocardial volume

(Fig. S1). Myocardial and hydrogel dimensions were acquired via MRI (Fig. S2, Table S1) and hydrogel moduli represent those determined by oscillatory rheology and compressive mechanical analysis for GH and DC hydrogels, respectively. Pressure (10 mmHg) was applied to the endocardial surface, mimicking that of end-diastolic relaxation and corresponding regional examination of myofiber stress was performed.

### Ovine infarct model

Animals in this study were provided care in compliance with the National Institute of Health's guidelines for the care and use of laboratory animals (NIH Publication 85–23, revised 1996) with protocol approval by the University of Pennsylvania's Institutional Animal Care and Use Committee. Twenty-two adult male Dorset sheep, approximately 45 kg, were subject to infarction and study up to 8 weeks.<sup>21</sup> Infarct size was determined by direct epicardial examination and quantification of LV and infarct area (ImageJ) at baseline and terminal timepoints, respectively; infarct size and animal weight were controlled across treatment groups (Table S2). For MI generation, sheep were induced (ketamine, 25 mg/kg), intubated, and maintained under anesthesia (isoflurane, 1.0–2.0%). A left thoracotomy was performed and a posterolateral infarct comprising approximately 20% of the LV was induced by selective ligation of the obtuse marginal (OM) branches (Fig. 1A). Thirty minutes post-ligation, sixteen injections (0.3 mL ea. via a 1/2cc syringe, with 27G ½" in needle) were performed in the infarct region, which consisted of saline (MI control), GH hydrogel, or DC hydrogel (Fig. 1B, C). The incision was closed in layers and the animal recovered under supervision with postoperative pain control (fentanyl, 25–75 µg, transdermal).

### Magnetic resonance imaging and analysis

Image acquisition was performed at 3T (Tim Magnetom Trio Scanner; Siemens, Inc.). For visualization of the hydrogels following *in vivo* injection, the explant was submerged in saline and imaged via a  $T_2$  weighted turbo spin echo pulse sequence. For longitudinal analysis of myocardial geometry and function *in vivo*, imaging was performed at baseline (immediately prior to infarct), as well as at 2 and 8 weeks post-infarct. Anesthesia was maintained throughout the procedure and cardiac gating was performed by placement of a pressure catheter (Millar Instruments, Inc.) into the LV. Myocardial geometry was assessed from two-dimensional CINE images, with additional late gadolinium enhancement (LGE) imaging to confirm the infarct location (Fig. S3). Imaging parameters and analysis methods are available in the supplementary methods.

### Post-mortem analysis

Animals were sacrificed at 8 weeks, the hearts harvested, and long-axis sections were taken through the infarct region (adjacent to the posterior papillary) and from remote sections (adjacent to the anterior papillary). From these samples, myocardial thickness was measured and reported as the average of three measurements from the base, infarct (approximately equatorial), and apex for each animal. Sections from these regions were fixed in formalin, paraffin embedded, and stained with Masson's Trichrome and hematoxylin and eosin (H&E). To evaluate the distribution of the hydrogel *in vivo*, tissue was analyzed in one GH and one DC hydrogel injected animal within the first 24 hours post-MI.

## Percutaneous intramyocardial injection

Two healthy adult male Dorsey sheep were utilized, allowing investigation of two separate procedural approaches, both utilizing a delivery system (Fig. S4) comprised of an Agilis™ NxT steerable introducer, a BRK™ transseptal needle (4 Fr, 90 cm; St. Jude Medical) pre-loaded intraoperatively with sterile hydrogel, and a 1 mL syringe containing the desired injection volume (0.3 mL each). Injection position was monitored by fluoroscopy and directly visualized by simultaneous intracardiac echocardiography (ICE; AcuNav 8 Fr, Siemens). In the first approach, the introducer was inserted through the internal jugular and passed into the right ventricle (RV) over wire. The sheath was deflected to reach various locations and the needle advanced 4–5 mm into the tissue for injection and subsequently retracted. Four injections were performed into the septal wall. In the second approach, the introducer was similarly passed into the LV with access via the right carotid, and five injections were performed into the inferior and anterior walls. Following the procedure, injection was confirmed by MRI of the explanted tissue.

## Statistical analysis

Data is presented as mean  $\pm$  standard deviation (SD, for *in vitro* data) or as mean  $\pm$  standard error of the mean (SEM, for *in vivo* data). Statistical significance was determined by ANOVA, using repeated measures where appropriate, in conjunction with post hoc Student's two-tailed t-tests with Bonferroni correction to account for multiple comparisons. Normality of data was confirmed by Shapiro-Wilk test. Significance was determined at  $\alpha = 0.05$ . For volumetric analysis, outliers were identified within groups by Grubb's test and excluded from further analysis.

## RESULTS

### Development of injectable hydrogels with controlled biophysical properties

GH hydrogel precursors were prepared with approximately 25% of HA repeat units modified with either Ad or CD. Upon mixing solutions of Ad-HA with CD-HA, GH hydrogels (Fig. 1B) rapidly formed through physical interactions. The elastic modulus (E) of GH hydrogels was estimated at 1.6 Hz (corresponding to a heart rate of 100 BPM) to be 799.2 Pa (Fig. S5A). GH hydrogels are known to exhibit shear-thinning (during injection) and self-healing (after injection) properties<sup>18,22</sup> necessary for delivery into myocardial tissue (Fig. 1D); yet, shear-yielding was not observed at physiological myocardial strains (Fig. S5B), indicating stability after reaching the tissue.

Dual-crosslinking (DC) hydrogels were developed to introduce additional covalent crosslinks into the GH hydrogels to increase their mechanical properties (Fig. 1C). Thus, they are likewise injectable via shear-thinning but with increased mechanical strength. DC hydrogels stiffened to  $41.4 \pm 4.3$  kPa moduli within 48 hours. Subsequent softening, significant beyond 2 weeks (Fig. 1E), was observed due to hydrogel degradation. GH and DC hydrogel degradation was monitored for 8 weeks (Fig. 1F); rapid degradation of the GH hydrogel was observed (>50% degradation), in contrast to the DC hydrogel, which remained stable up to 8 weeks ( $5.1 \pm 0.2\%$  degradation).

*In vivo* examination of hydrogel retention was performed at 24 hours following infarct induction and intramyocardial injection. Both the GH and DC hydrogels were retained as solid, discrete hydrogels within the myocardium (Fig. 2A,B). MRI of DC hydrogel injection (Fig. 2C) demonstrated dispersion of hydrogel throughout the tissue with a measured volume of 5.1 mL, in agreement with the 4.8 mL of hydrogel injected. Excised DC hydrogels exhibited moduli of  $30.3 \pm 2.6$  kPa, coinciding with measured *in vitro* moduli at these times ( $P=0.83$ ) and demonstrating the ability for dual-crosslinking to occur *in vivo*.

### Finite element assessment of myofiber stress and LV wall deformation

FE simulations were conducted to evaluate anticipated myocardial bulking and altered distribution of end-diastolic myofiber stress throughout the LV wall at early times post-MI. The end-diastolic wall thickness within the injected regions differed between the control, GH, and DC cases ( $1.01 \pm 0.025$ ,  $1.08 \pm 0.029$ , and  $1.23 \pm 0.023$  cm,  $P < 0.09 \times 10^{-2}$ ). Qualitatively, the myofiber stress distributions throughout the LV were differentially altered by GH (Fig. 3A) and DC (Fig. 3B) hydrogel injections. The average stress in the myocardium surrounding the DC injection was  $2.5 \pm 0.13$  kPa (27.0 $\pm$ 8.0% reduction relative to control,  $P < 0.0001$ ), while the stress around the GH injection was  $3.4 \pm 0.28$  kPa ( $P=NS$ ; Fig. 3C). Through the transmural dimension, DC injection reduced the myofiber stress by 45.0 $\pm$ 1.6 % at the epicardium, 26.1 $\pm$ 4.5% at mid-myocardium, and 51.4 $\pm$ 3.0% at the endocardium compared to the control case ( $P < 0.42 \times 10^{-6}$ , Fig. 3D). Circumferentially, near the edge of the injection region, hydrogels reduced the myofiber stress (Fig. 3E) by a maximum of 31.5 $\pm$ 8.8% for GH ( $P=0.16 \times 10^{-6}$ ) and 62.0 $\pm$ 4.4% for DC ( $P=0.55 \times 10^{-6}$ ), relative to controls.

### Assessment of myocardial thickness

Wall thickness was measured following excision at 8 weeks. Qualitatively, thinning of the infarct region was observed after MI (Fig. 4A) which was attenuated by hydrogel injection and remaining DC hydrogel was observed post-mortem in all cases. Histological examination (Fig. S7,8) indicated integration of the DC hydrogel into the tissue, which was not apparent at early timepoints (Fig. 2B), with minimal chronic inflammation (i.e. foreign-body giant cell localization, fibrous encapsulation). Histologically, GH materials were not observed at 8 weeks, consistent with the observed rapid erosion (Fig. 1F) and prior *in vivo* examination.<sup>19</sup> Quantitatively, hydrogel injection increased infarct thickness relative to controls (MI:  $3.90 \pm 0.48$  mm; GH:  $5.79 \pm 0.96$  mm,  $P=0.013$ ; DC:  $8.92 \pm 0.24$  mm,  $P=0.46 \times 10^{-6}$ ) and tended to increase adjacent basilar and apical thicknesses (Fig. 4B, Table S3). Temporal assessment of end-diastolic thickness by MRI (Fig. 4C) revealed significant differences between infarct tissue thickness at 2 and 8 weeks, with minimal differences observed in remote thicknesses (Table S4). Notably, DC hydrogel injection was observed to maintain wall thickness at 8 weeks ( $10.02 \pm 0.79$  mm;  $P > 0.35$  relative to baseline), in contrast to the observed drastic thinning in both MI ( $3.56 \pm 0.19$  mm;  $P=0.67 \times 10^{-12}$ ) and GH ( $5.51 \pm 0.23$  mm;  $P=0.24 \times 10^{-8}$ ) groups.

### LV dilation and functional assessment

MRI was utilized to assess temporal changes in LV volume and function. The LV progressively dilated, as indicated by a greater than two-fold increase ( $P < 0.014$  relative to



baseline) in LVEDV and LVESV in MI controls. At end-diastole (Fig. 5A), hydrogel treatment tended toward reduced dilation at 8 weeks. Significant differences were observed between DC and MI at 2 weeks, and between DC and both GH and MI groups at 8 weeks at end-systole (Fig. 5B). While not significant, SV (Fig. 5C) was increased with DC hydrogel injection. EF (Fig. 5D) showed a consistent, progressive loss of function following MI, which was moderately attenuated by GH (15% improvement,  $P=0.058$ ) and significantly attenuated by DC (37% improvement,  $P=0.014$ ) hydrogel injections at 8 weeks.

### Percutaneous hydrogel delivery

The potential for percutaneous injection of the shear-thinning GH hydrogel was examined using equipment and methods amenable to adaptation in the majority of interventional cardiology units. Hydrogels were prepared as described, and the injection volume (0.3 mL) was loaded into 1 mL Luer-Lock syringes. The desired injection location (i.e., septal for RV approach, anterior and posterior wall for LV approach) were identified by fluoroscopy, the introduction sheath positioned, and ICE used to allow visualization of the needle location (Fig. 6 A,D). Injections were performed by insertion of needle into the LV wall, as visualized by ICE (Fig. 6A, inset). Following sacrifice and excision of the heart, hydrogel injections were visualized by MRI. As with syringe injection, discrete hydrogel injections were located along the long axis (Fig. 6 B,E) and short axis (Fig. 6 C,F) of the myocardium.

### Discussion

Toward abating LV remodeling post-MI, epicardial placement of devices, including both mechanical restraints<sup>10</sup> and therapeutic-containing patches<sup>23,24</sup> have demonstrated great efficacy in pre-clinical studies. However, the clinical application of such therapies will likely be limited due to their inherent requirement for open surgical approaches. To address this important consideration, therapeutics that may be delivered via catheter have been investigated (i.e., cell therapy).<sup>25</sup> In addition to such approaches, our group and others have utilized a combination of experimental and computational tactics to explore the capacity for injectable hydrogels to directly alter the mechanical environment both in and around the infarcted region.<sup>9,12,13,20,26</sup>

The ability of material injection to reduce myofiber stress within the infarct region and its borderzone is critical, as rapid geometric changes within the infarct (i.e. infarct expansion) and progressive dysfunction of the borderzone have been repeatedly implicated in progression of LV remodeling. GH and DC hydrogels are both shear-thinning and self-healing to permit hydrogel localization in the myocardium (Fig. 2, S5); however, the DC hydrogel exhibits stiffening (>40-fold change) to increase the hydrogel mechanical properties. DC injection showed greater reduction in myofiber stress, relative to MI controls with FE modeling. For DC injections, stress reduction was driven by the preservation of LV shape by maintaining the LV wall thickness. In contrast, GH injections deformed under loading, elongating circumferentially (Fig. 3A). Although only an initial snapshot into this mechanism, these results indicate that the hydrogel stiffness is important because it enables reduction in fiber stress through stiffness-induced bulking of the myocardium. While progressive DC degradation resulted in moduli decline and hydrogel integration with the

host tissue, the therapy is intended to intercept the remodeling process early after infarction and prior to endogenous infarct stiffening which occurs later due to collagen deposition.<sup>27</sup>

Myocardial bulking predicted by FE modeling was consistent with *in vivo* observations, as the thickness of the myocardium was better maintained with hydrogel injection. Notably, DC injection maintained baseline measurements at 2 and 8 weeks ( $P > 0.35$  relative to baseline). Importantly, recent analyses have highlighted myocardial thinning as a dominant feature of LV remodeling, consistent across species, making it an attractive therapeutic target.<sup>28</sup> In addition to bulking, the FE model predicted alterations in myocardial loading which translated to attenuation of LV remodeling events *in vivo*, with DC treatment resulting in significant reduction in LVESV and improvement in EF at both 2 and 8 weeks. Both of these metrics have been shown to be valuable clinical predictors for survival post-MI.<sup>29,30</sup> While decreased LV volume, resulting from tissue displacement by hydrogel, may contribute minimally to changes in EF, the injection volumes alone (4.8 mL) cannot account for the disparity in LVES volumes between control and DC cases ( $44.0 \pm 12.8$  mL at 8 wk) and consistent improvement in SV was demonstrated, indicating genuine preservation of both ventricular geometry and function.

To enable formation of injectable hydrogels *in vivo* for MI applications, both physical and covalent crosslinking have been individually leveraged.<sup>11</sup> Yet, only physically crosslinked hydrogels have been delivered percutaneously via catheters. Specifically, calcium crosslinked alginate has been delivered via intracoronary infusion<sup>14</sup> and decellularized extracellular matrix<sup>15,31</sup> and pH responsive poly(ethylene glycol) assemblies<sup>16</sup> have been delivered via intramyocardial injection. For such physically assembling systems, the range of attainable elastic moduli limit their applicability toward mechanical restraint.<sup>32</sup> Yet, positive results have been demonstrated in porcine models, possibly attributable to biological effects,<sup>33</sup> and these material systems have advanced to clinical trials (AUGMENT-HF, VentiGel).

While physically assembling systems have demonstrated percutaneous delivery with some positive effects on LV remodeling, they have failed to exploit mechanical stabilization in their mechanism of action. Alternatively, covalent crosslinking of hydrogels has been utilized to achieve mechanical restraint of the infarcted region, with increasing stiffness and prolonged degradation correlated with improved functional outcomes.<sup>12,13</sup> However, gelation of these systems relies on the mixing of several components, which can be challenging with a catheter where rapid gelation can clog the catheter and slow gelation can lead to material dispersion in the tissue, compromising hydrogel formation.<sup>19</sup> This challenge has prevented covalently crosslinking hydrogels from being delivered percutaneously.

To address these limitations, we leveraged physical interactions (i.e., guest-host complexes) to enable formation of a soft hydrogel which exhibited fluid-like behavior within the needle or catheter to allow injection. Importantly, the GH hydrogels allowed rapid re-assembly within the tissue and thus high local retention (Fig. 2). Similar to the previously mentioned soft materials (e.g., alginate, decellularized ECM), there was some positive outcomes with the soft GH hydrogel — likely due to the biological effect of injecting a foreign material into the myocardium, which may alter collagen production. Secondary covalent crosslinking, via



thiol-ene addition reaction, has been tuned to provide crosslinking on the order of hours under controlled conditions (i.e., pH 5), to enable ease of use in a clinical setting.<sup>19</sup> The resulting stiffer DC hydrogels provided tissue bulking to thicken the myocardium, reduce myofiber stress, and attenuate LV remodeling. Taken together, we have developed a catheter-injectable material system with the ability to mitigate LV remodeling through mechanical restraint afforded by the stiff hydrogel.

The present study has demonstrated that hydrogels can effectively assuage LV remodeling after MI without the need for added therapeutics (i.e. cells, drugs) through modulation of the myocardial stresses. The study also demonstrated the feasibility of delivering these materials via catheter-based techniques, due to the independently designed mechanisms for material retention and stiffening. Such materials will facilitate the development of clinically relevant approaches, owing to the relative ease of preparation and potential for minimally invasive delivery.<sup>10, 11, 34</sup> Moreover, the primary constituents (i.e., HA and CD) are generally recognized as safe (GRAS) by the US Food and Drug Administration and are industrially well represented in the pharmaceutical and medical device industries.<sup>35, 36</sup> The defined material formulations therefore constitute a medical device that holds potential to rapidly progress toward clinical use.

Despite the positive findings, it is important to address potential limitations in the study. Intervention with hydrogel injection was performed at the time of infarct induction; though, intervention in the 3 to 7 day range may be more clinically feasible (Bellerophon, [ClinicalTrials.gov](https://clinicaltrials.gov/ct2/show/study/NCT01226563) Identifier: NCT01226563). The results of this study therefore demonstrate the capacity for the material systems developed to act as a preventative therapy to alter LV remodeling, as well a delivery approach that could expand the feasibility of injection at later times. While efficacy of material injection at later time points has been demonstrated in both animal<sup>31, 37, 38</sup> and clinical studies,<sup>39</sup> the optimization of injection time for both clinical applicability and efficacy remains an important issue in need of direct examination. These efforts will be aided by percutaneous injection procedures that are accompanied by myocardial mapping. Additionally, animals were only studied out to 8 weeks post-MI; longer studies will be required to assess the durability of the therapeutic response at time points beyond the *in vivo* lifetime of the DC materials. Ultimately, translation of the materials described here will be dependent on future studies that will be focused on timing, dosing, and injection location.

## Conclusion

For the first time, we have developed shear-thinning hydrogels with therapeutically relevant properties for delivery via percutaneous intramyocardial injection. Such shear-thinning delivery enabled local hydrogel retention, while secondary covalent crosslinking enhanced mechanically advantageous bulking of the infarct tissue. Importantly, the stiffening reaction occurred autonomously *in situ* on clinically relevant timescales and further enhanced treatment efficacy through bulking and mechanical stabilization of the infarct. The dual-crosslinking hydrogel system represents the first engineered material designed to specifically and simultaneously address the needs of localized retention, mechanical stabilization, and

percutaneous delivery for treatment of MI. The present study establishes the efficacy of the material system as a therapeutic approach toward moderating LV remodeling.

## Supplementary Material

Refer to Web version on PubMed Central for supplementary material.

## Acknowledgments

The authors thank the Gorman Cardiovascular Research Group members including Nicole Peranteau, Christen Dillard, Jerry Zsido, Madeline Vind, and Sabrina Leventhal for assistance in completion of the animal model.

### Sources of Funding

This work was financially supported by the NIH (R01 HL063954, R01 HL111090). Dr. Rodell and Dr. Burdick hold a Predoctoral Fellowship and Established Investigator Award from the American Heart Association, respectively.

## References

1. Mozaffarian D, Benjamin EJ, Go AS, Arnett DK, Blaha MJ, Cushman M, de Ferranti S, Despres J-P, Fullerton HJ, Howard VJ. Heart disease and stroke statistics-2015 update: A report from the American Heart Association. *Circulation*. 2015; 131:e29. [PubMed: 25520374]
2. Peterson ED, Shah BR, Parsons L, Pollack CV, French WJ, Canto JG, Gibson CM, Rogers WJ, Investigators N. Trends in quality of care for patients with acute myocardial infarction in the national registry of myocardial infarction from 1990 to 2006. *Am. Heart J.* 2008; 156:1045–1055. [PubMed: 19032998]
3. Jessup M, Brozena S. Medical progress: Heart failure. *N. Engl. J. Med.* 2003; 348:2007–2018. [PubMed: 12748317]
4. Holmes JW, Borg TK, Covell JW. Structure and mechanics of healing myocardial infarcts. *Annual review of biomedical engineering*. 2005:223–253.
5. Spinale FG. Myocardial matrix remodeling and the matrix metalloproteinases: Influence on cardiac form and function. *Physiol. Rev.* 2007; 87:1285–1342. [PubMed: 17928585]
6. Gupta KB, Ratcliffe MB, Fallert MA, Edmunds LH, Bogen DK. Changes in passive mechanical stiffness of myocardial tissue with aneurysm formation. *Circulation*. 1994; 89:2315–2326. [PubMed: 8181158]
7. Vanhoutte D, Schellings M, Pinto Y, Heymans S. Relevance of matrix metalloproteinases and their inhibitors after myocardial infarction: A temporal and spatial window. *Cardiovasc. Res.* 2006; 69:604–613. [PubMed: 16360129]
8. Jackson BM, Gorman JH, Moainie SL, Guy TS, Narula N, Narula J, John-Sutton MGS, Edmunds LH, Gorman RC. Extension of borderzone myocardium in postinfarction dilated cardiomyopathy. *J Am Coll Cardiol.* 2002; 40:1160–1167. [PubMed: 12354444]
9. Wall ST, Walker JC, Healy KE, Ratcliffe MB, Guccione JM. Theoretical impact of the injection of material into the myocardium - a finite element model simulation. *Circulation*. 2006; 114:2627–2635. [PubMed: 17130342]
10. Gorman RC, Jackson BM, Burdick JA, Gorman JH. Infarct restraint to limit adverse ventricular remodeling. *J Cardiovasc Transl.* 2011; 4:73–81.
11. Tous E, Purcell B, Ifkovits JL, Burdick JA. Injectable acellular hydrogels for cardiac repair. *J Cardiovasc Transl.* 2011; 4:528–542.
12. Ifkovits JL, Tous E, Minakawa M, Morita M, Robb JD, Koomalsingh KJ, Gorman JH, Gorman RC, Burdick JA. Injectable hydrogel properties influence infarct expansion and extent of postinfarction left ventricular remodeling in an ovine model. *Proc. Natl. Acad. Sci. U.S.A.* 2010; 107:11507–11512. [PubMed: 20534527]

13. Tous E, Ifkovits JL, Koomalsingh KJ, Shuto T, Soeda T, Kondo N, Gorman JH, Gorman RC, Burdick JA. Influence of injectable hyaluronic acid hydrogel degradation behavior on infarction-induced ventricular remodeling. *Biomacromolecules*. 2011; 12:4127–4135. [PubMed: 21967486]
14. Leor J, Tuvia S, Guetta V, Manczur F, Castel D, Willenz U, Petnehazy O, Landa N, Feinberg MS, Konen E, Goitein O, Tsur-Gang O, Shaul M, Klapper L, Cohen S. Intracoronary injection of in situ forming alginate hydrogel reverses left ventricular remodeling after myocardial infarction in swine. *J Am Coll Cardiol*. 2009; 54:1014–1023. [PubMed: 19729119]
15. Singelyn JM, Sundaramurthy P, Johnson TD, Schup-Magoffin PJ, Hu DP, Faulk DM, Wang J, Mayle KM, Bartels K, Salvatore M, Kinsey AM, DeMaria AN, Dib N, Christman KL. Catheter-deliverable hydrogel derived from decellularized ventricular extracellular matrix increases endogenous cardiomyocytes and preserves cardiac function post-myocardial infarction. *J Am Coll Cardiol*. 2012; 59:751–763. [PubMed: 22340268]
16. Bastings M, Koudstaal S, Kieltyka RE, Nakano Y, Pape A, Feyen DA, van Slochteren FJ, Doevendans PA, Sluijter JP, Meijer E. A fast ph-switchable and self-healing supramolecular hydrogel carrier for guided, local catheter injection in the infarcted myocardium. *Adv. Healthcare Mater*. 2014; 3:70–78.
17. Johnson TD, Lin SY, Christman KL. Tailoring material properties of a nanofibrous extracellular matrix derived hydrogel. *Nanotechnology*. 2011; 22:494015. [PubMed: 22101810]
18. Rodell CB, Kaminski AL, Burdick JA. Rational design of network properties in guest-host assembled and shear-thinning hyaluronic acid hydrogels. *Biomacromolecules*. 2013; 14:4125–4134. [PubMed: 24070551]
19. Rodell CB, MacArthur JW, Dorsey SM, Wade RJ, Wang LL, Woo YJ, Burdick JA. Shear-thinning supramolecular hydrogels with secondary autonomous covalent crosslinking to modulate viscoelastic properties in vivo. *Adv. Funct. Mater*. 2015; 25:636–644. [PubMed: 26526097]
20. Kichula ET, Wang H, Dorsey SM, Szczesny SE, Elliott DM, Burdick JA, Wenk JF. Experimental and computational investigation of altered mechanical properties in myocardium after hydrogel injection. *Ann Biomed Eng*. 2014; 7:1546–1556.
21. Gorman JH, Gorman RC, Plappert T, Jackson BM, Hiramatsu Y, John-Sutton MGS, Edmunds LH. Infarct size and location determine development of mitral regurgitation in the sheep model. *J Thorac Cardiovasc Surg*. 1998; 115:615–622. [PubMed: 9535449]
22. Rodell CB, Mealy JE, Burdick JA. Supramolecular guest–host interactions for the preparation of biomedical materials. *Bioconjugate Chem*. 2015; 26:2279–2289.
23. Miyagi Y, Chiu LLY, Cimini M, Weisel RD, Radisic M, Li RK. Biodegradable collagen patch with covalently immobilized vegf for myocardial repair. *Biomaterials*. 2011; 32:1280–1290. [PubMed: 21035179]
24. Purcell BP, Elser JA, Mu AB, Margulies KB, Burdick JA. Synergistic effects of sdf-1 alpha chemokine and hyaluronic acid release from degradable hydrogels on directing bone marrow derived cell homing to the myocardium. *Biomaterials*. 2012; 33:7849–7857. [PubMed: 22835643]
25. Sherman W, Martens TP, Viles-Gonzalez JF, Siminiak T. Catheter-based delivery of cells to the heart. *Nat. Clin. Pract. Cardiovasc. Med*. 2006; 3:S57–S64. [PubMed: 16501633]
26. Dorsey SM, McGarvey JR, Wang H, Nikou A, Arama L, Koomalsingh KJ, Kondo N, Gorman JH, Pilla JJ, Gorman RC. Mri evaluation of injectable hyaluronic acid-based hydrogel therapy to limit ventricular remodeling after myocardial infarction. *Biomaterials*. 2015; 69:65–75. [PubMed: 26280951]
27. Fomovsky GM, Holmes JW. Evolution of scar structure, mechanics, and ventricular function after myocardial infarction in the rat. *Am J Physiol-Heart C*. 2010; 298:H221–H228.
28. Richardson W, Holmes J. Why is infarct expansion such an elusive therapeutic target? *J Cardiovasc Transl*. 2015:421–430.
29. White HD, Norris R, Brown MA, Brandt P, Whitlock R, Wild C. Left ventricular end-systolic volume as the major determinant of survival after recovery from myocardial infarction. *Circulation*. 1987; 76:44–51. [PubMed: 3594774]
30. Solomon SD, Anavekar N, Skali H, McMurray JJ, Swedberg K, Yusuf S, Granger CB, Michelson EL, Wang D, Pocock S. Influence of ejection fraction on cardiovascular outcomes in a broad spectrum of heart failure patients. *Circulation*. 2005; 112:3738–3744. [PubMed: 16330684]

31. Seif-Naraghi SB, Singelyn JM, Salvatore MA, Osborn KG, Wang JJ, Sampat U, Kwan OL, Strachan GM, Wong J, Schup-Magoffin PJ. Safety and efficacy of an injectable extracellular matrix hydrogel for treating myocardial infarction. *Sci. Transl. Med.* 2013; 5 173ra125-173ra125.
32. Venugopal JR, Prabhakaran MP, Mukherjee S, Ravichandran R, Dan K, Ramakrishna S. Biomaterial strategies for alleviation of myocardial infarction. *J R Soc Interface.* 2012; 9:1–19. [PubMed: 21900319]
33. Seif-Naraghi SB, Salvatore MA, Schup-Magoffin PJ, Hu DP, Christman KL. Design and characterization of an injectable pericardial matrix gel: A potentially autologous scaffold for cardiac tissue engineering. *Tissue Eng., Part A.* 2010; 16:2017–2027. [PubMed: 20100033]
34. Burdick JA, Mauck RL, Gorman JH, Gorman RC. Acellular biomaterials: An evolving alternative to cell-based therapies. *Sci. Transl. Med.* 2013; 5 176ps4.
35. Highley CB, Prestwich GD, Burdick JA. Recent advances in hyaluronic acid hydrogels for biomedical applications. *Curr. Opin. Biotechnol.* 2016; 40:35–40. [PubMed: 26930175]
36. Szejtli J. Introduction and general overview of cyclodextrin chemistry. *Chem. Rev.* 1998; 98:1743–1753. [PubMed: 11848947]
37. Landa N, Miller L, Feinberg MS, Holbova R, Shachar M, Freeman I, Cohen S, Leor J. Effect of injectable alginate implant on cardiac remodeling and function after recent and old infarcts in rat. *Circulation.* 2008; 117:1388–1396. [PubMed: 18316487]
38. Yoshizumi T, Zhu Y, Jiang H, D'Amore A, Sakaguchi H, Tchao J, Tobita K, Wagner WR. Timing effect of intramyocardial hydrogel injection for positively impacting left ventricular remodeling after myocardial infarction. *Biomaterials.* 2016; 83:182–193. [PubMed: 26774561]
39. Lee LC, Wall ST, Klepach D, Ge L, Zhang ZH, Lee RJ, Hinson A, Gorman JH, Gorman RC, Guccione JM. Algisyl-lvr (tm) with coronary artery bypass grafting reduces left ventricular wall stress and improves function in the failing human heart. *Int. J. Cardiol.* 2013; 168:2022–2028. [PubMed: 23394895]

**WHAT IS KNOWN**

- Left ventricular (LV) remodeling and heart failure following myocardial infarction are characterized by progressive ventricular dilation and decreased ejection fraction (EF).
- Mechanical restraints, including myocardial wraps and injectable biomaterials, may attenuate LV remodeling.

**WHAT THE STUDY ADDS**

- This report describes the development of two distinct injectable materials with differing stiffness and degradation times, where ventricular dilation and loss of EF are most attenuated by the stiff and slowly degrading material in a large animal model.
- Finite element modeling demonstrates bulking of the myocardial wall and reduction of potentially damaging myofiber stress both within and surrounding the infarct, dependent upon material stiffness.
- Percutaneous intramyocardial injection of the materials is feasible, as demonstrated with catheter guidance by fluoroscopy and intracardiac echocardiography.

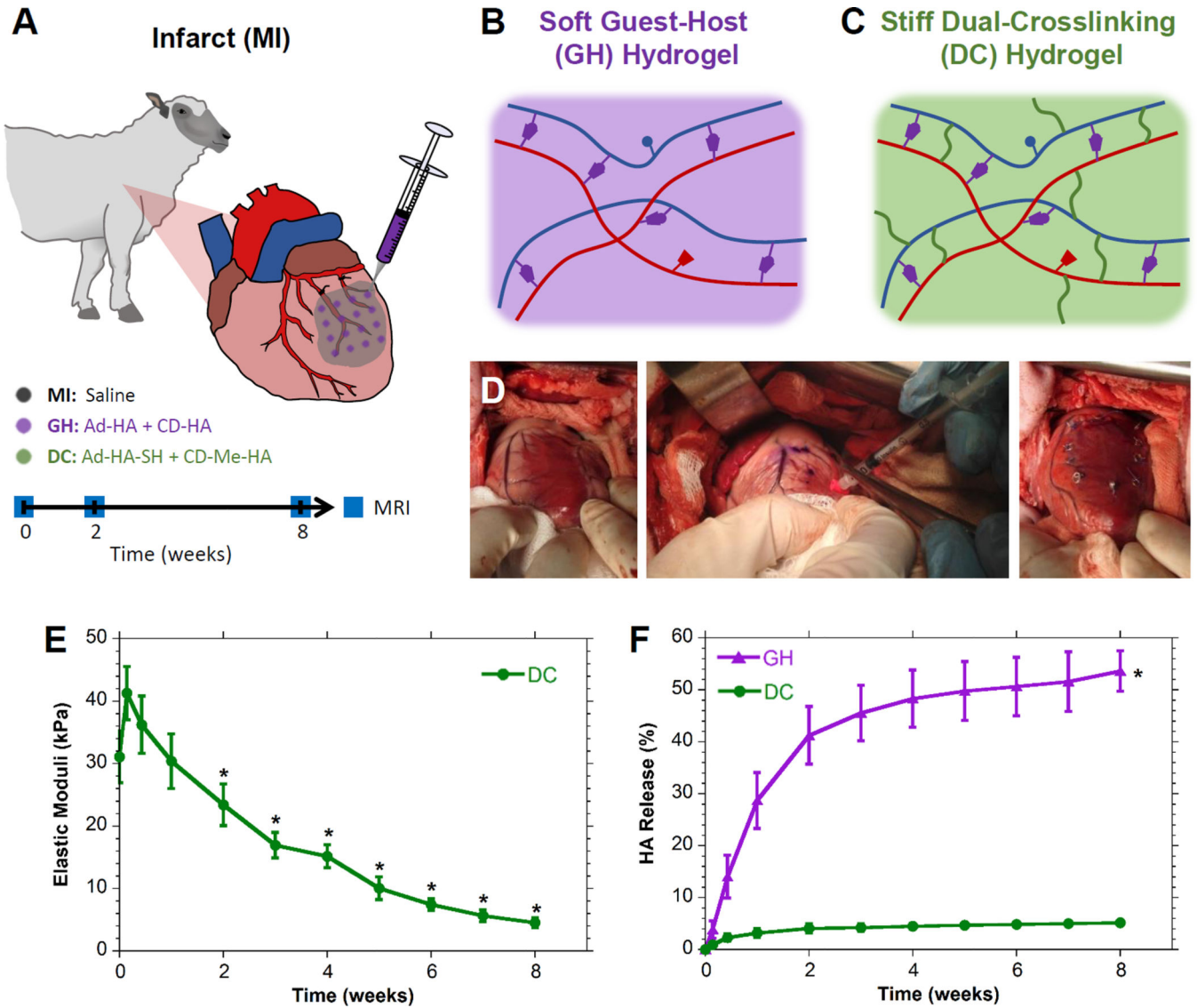


**Figure 1.** MI Model and Therapeutic Groups. **A**, Infarct generation by selective obtuse marginal ligation and injection with saline (MI control), guest-host hydrogel (GH), or dual-crosslinking hydrogel (DC) which were longitudinally assessed by MRI. **B**, GH hydrogels were composed of adamantane modified hyaluronic acid (Ad-HA, blue) and cyclodextrin modified hyaluronic acid (CD-HA, red) which form physical associations (purple). **C**, DC hydrogels were composed of thiolated Ad-HA (Ad-HA-SH) and methacrylated CD-HA (CD-MeHA), and resulted in additional covalent crosslinks (green). **D**, Both GH and DC hydrogels were injected into the infarcted region. **E**, DC hydrogel elastic moduli over time (mean±SD; n = 6; \*P < 0.01 relative to day 0). GH moduli are excluded, due to swelling which prevented reliable rheological testing over time. **F**, Hydrogel degradation (mean±SD with error bars for all points (not visible for DC); n = 5; \*P < 0.05 relative to DC for all timepoints beyond day 1).

Author Manuscript

Author Manuscript

Author Manuscript

Author Manuscript



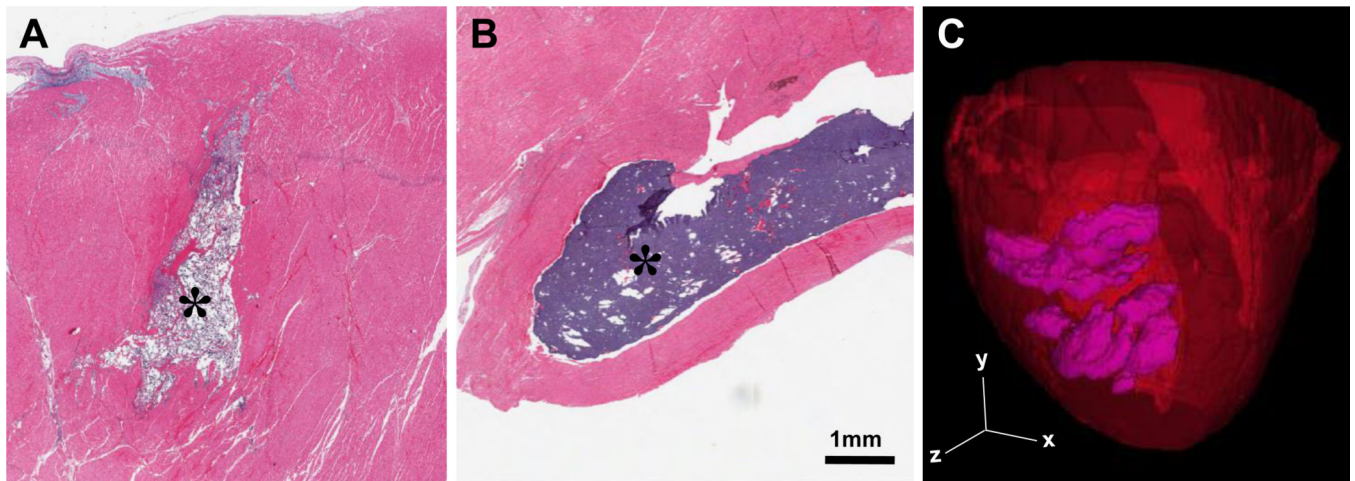


**Figure 2.** Material Retention In Vivo. **A-B**, Histological image of GH (**A**) and DC (**B**) hydrogels (indicated, \*) within infarct tissue by H&E staining at 1 day post-MI. For complete image and corresponding trichrome staining, see Fig. S6. **C**, MRI reconstruction of retained DC hydrogel (purple) within the myocardium (red) following initial injection *in vivo*.

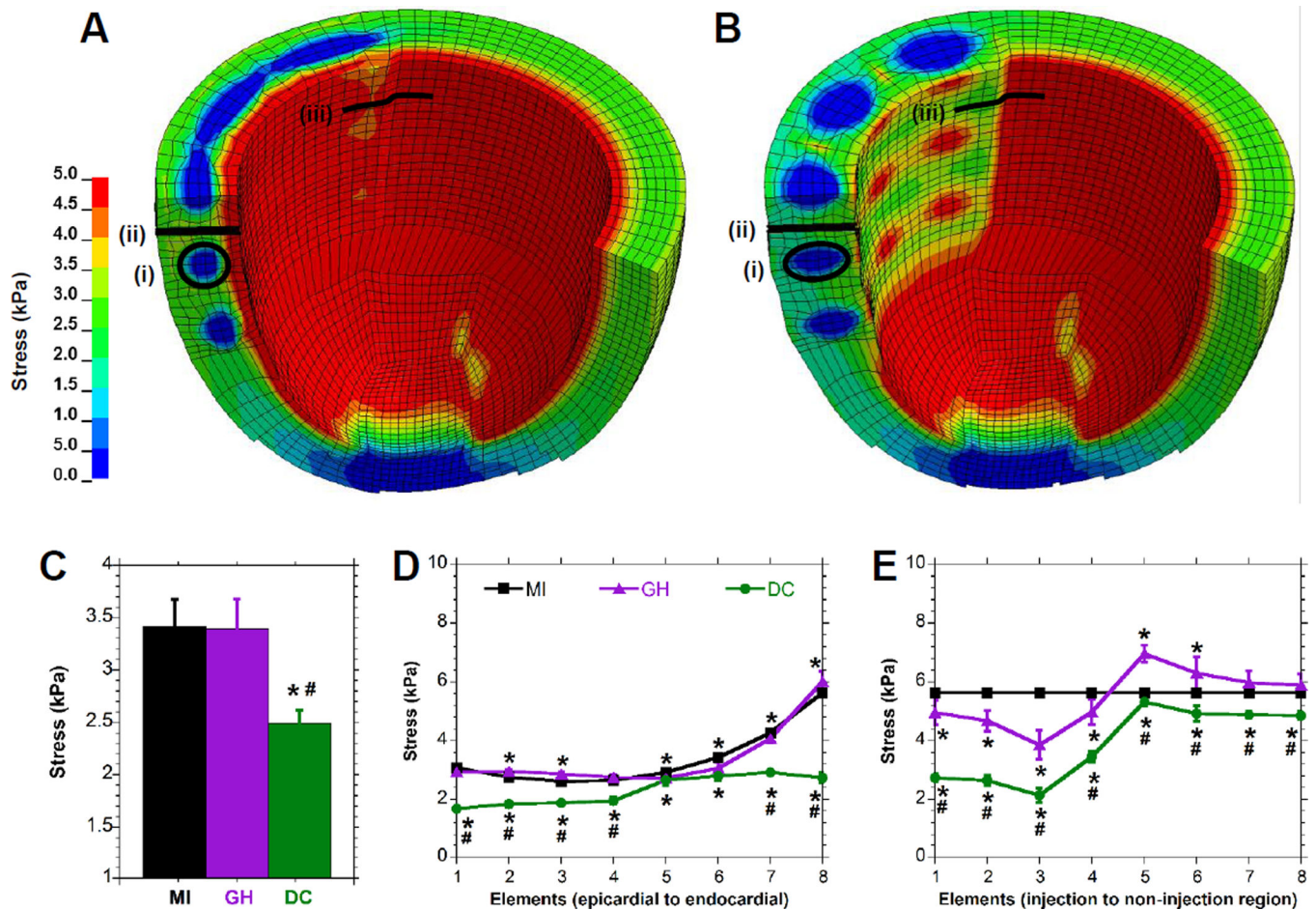


**Figure 3.** Finite Element Analysis of Hydrogel Injection. **A-B**, End-diastolic myofiber stress distribution for an LV with either (A) GH hydrogel injection or (B) DC hydrogel injection. Note that only a portion of the model is shown in order to visualize the distribution within the myocardium. **C-E**, Myofiber stress in elements adjacent to the material (C), or distributed along a transmural (D) or circumferential (E) path in the edge of the injection region. Corresponding regions are indicated for the material region (i) or transmural (ii) and circumferential (iii) paths. Data are presented as mean±SD with error bars for all points (some not visible due to low error); n = 6; \*P < 0.05 relative to MI; #P < 0.05 relative to GH.

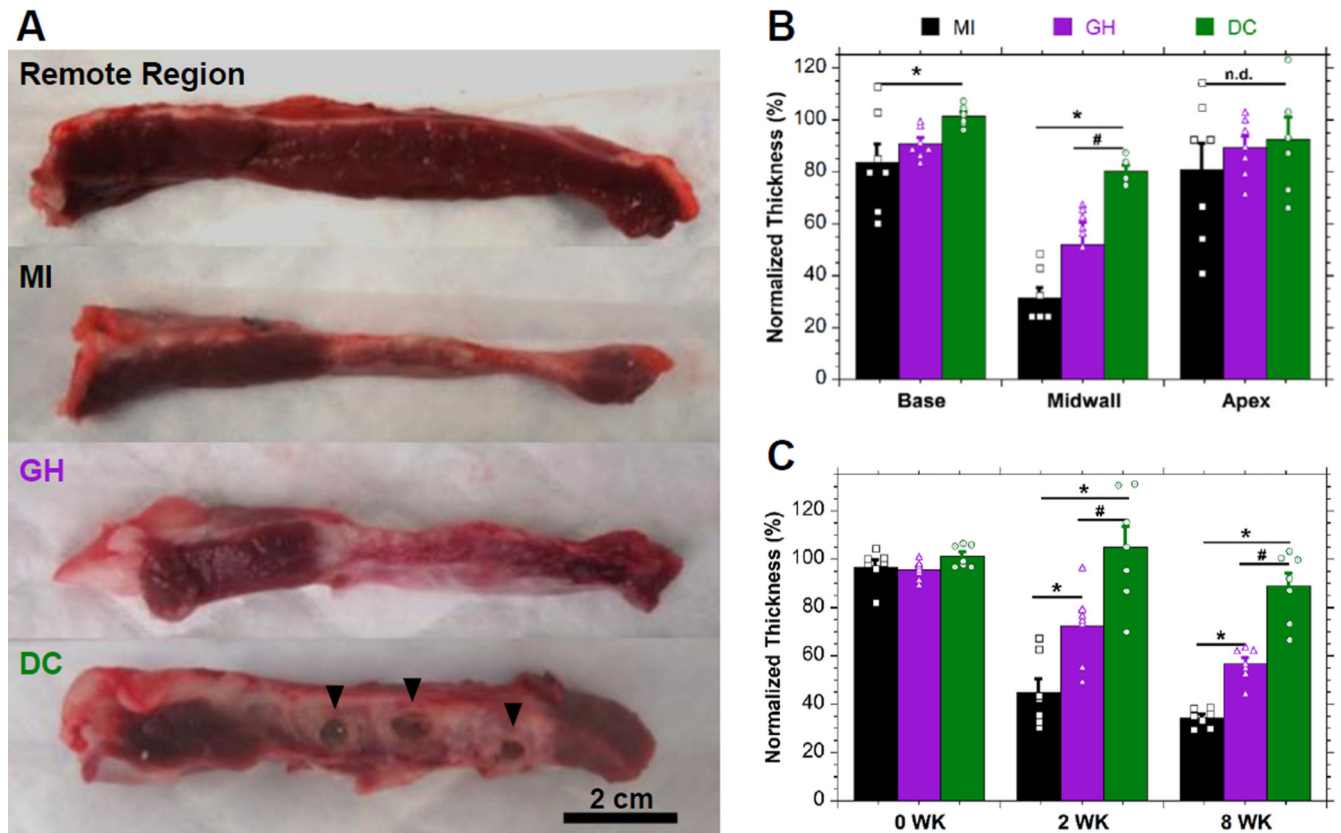


**Figure 4.** Myocardial Wall Thickness. **A**, Macroscopic images of remote or infarcted regions with hydrogel indicated (▼) for DC treatment. **B**, Corresponding thickness quantification. **C**, Temporal assessment of infarct thickness by MRI. Measurements are normalized to remote sections (mean±SEM; n = 6; \*P < 0.05 relative to MI; #P < 0.05 relative to GH).

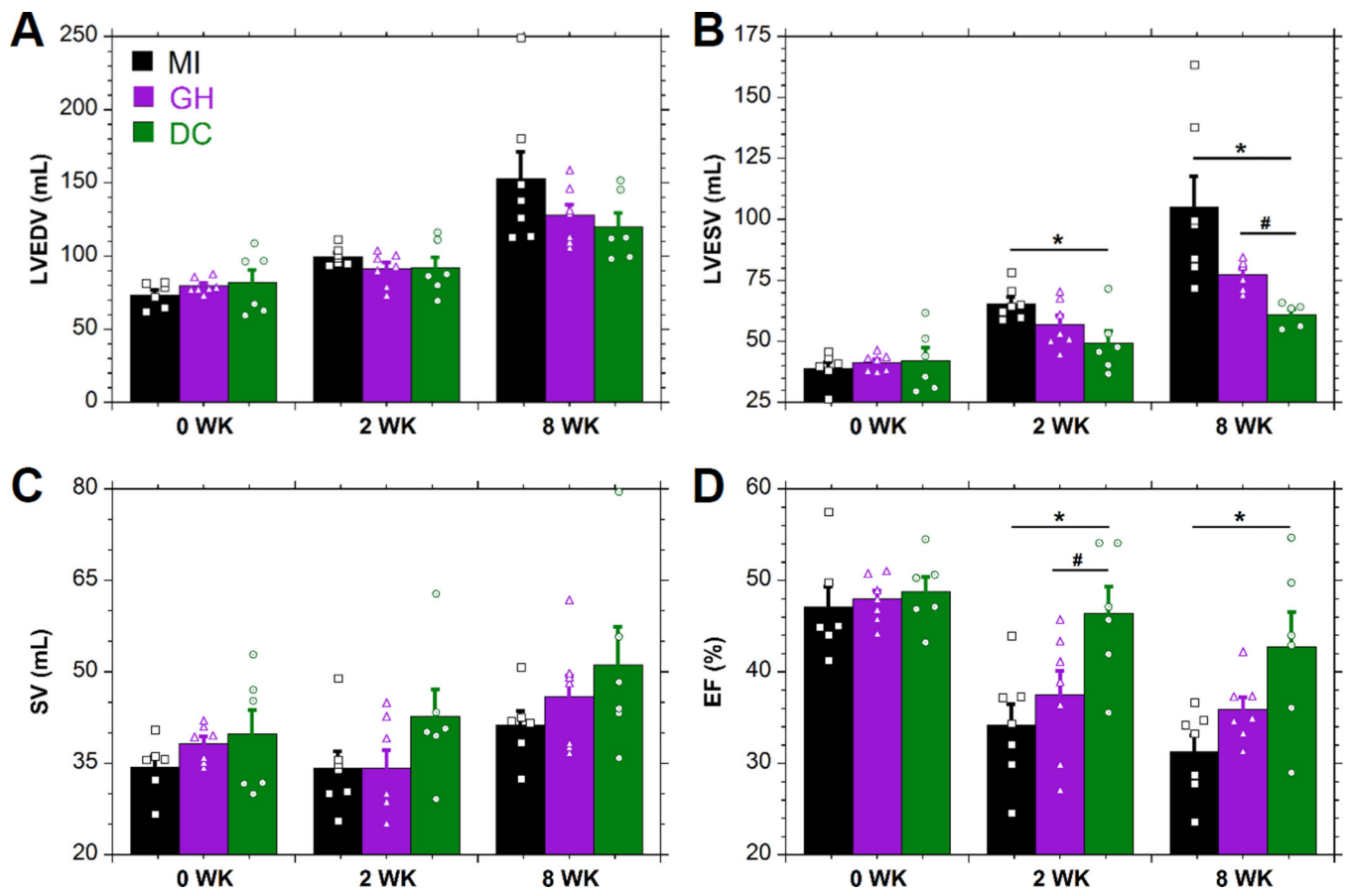


**Figure 5.** MRI Assessment of Cardiac Geometry and Function. MRI determination of LVEDV (A), LVESV (B), SV (C), and EF (D) (mean±SEM; n 6; \*P < 0.05 relative to MI; #P < 0.05 relative to GH).



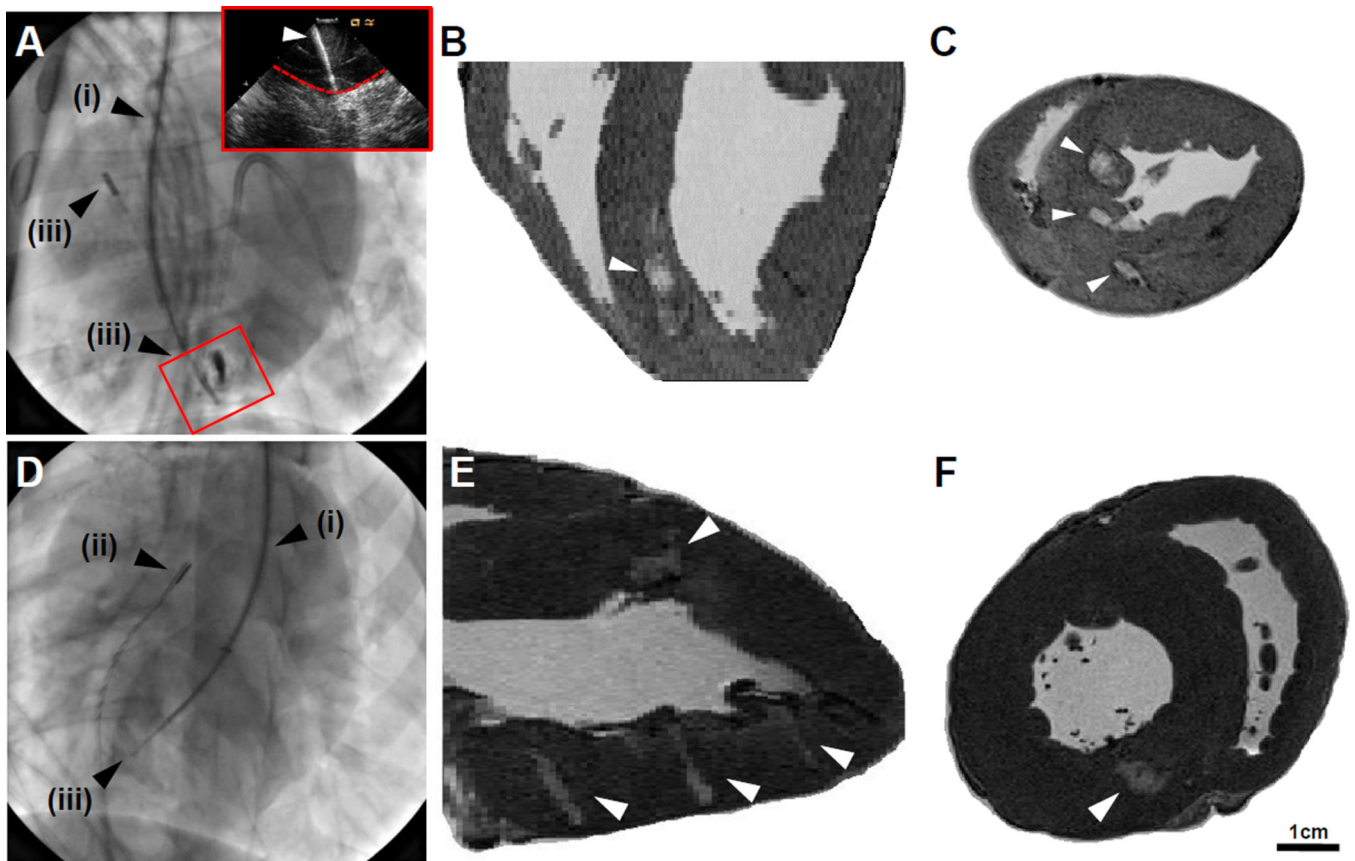


**Figure 6.** Percutaneous Hydrogel Injection. **A**, Internal jugular approach toward RV injection, with alignment of the steerable introducer (**i**), intracardiac echocardiograph probe (ICE, **ii**), and deployment of needle assembly (**iii**). Inset: corresponding ICE view of deployed needle (indicated, white arrow) entering the myocardial wall (indicated, dashed red line). **B-C**, Long axis (**B**) and short axis (**C**) images of hydrogel injection (indicated, white arrows). **D**, Right carotid approach toward LV injection, including steerable introducer (**i**), ICE (**ii**), and deployment of needle assembly (**iii**) into the midwall of the LV. **E-F**, Long axis (**E**) and short axis (**F**) images of hydrogel (indicated, white arrows).